# Inhibition of acute lethal pulmonary inflammation by the IDO–AhR pathway

Soung-Min Lee[a], Ha Young Park[a], Young-Sill Suh[a], Eun Hye Yoon[a], Juyang Kim[b], Won Hee Jang[c], Won-Sik Lee[d], Sae-Gwang Park[a], Il-Whan Choi[a], Inhak Choi[a,e], Sun-Woo Kang[f], Hwayoung Yun[g], Takanori Teshima[h], Byungsuk Kwon[b], and Su-Kil Seo[a,1]

[a]Department of Microbiology and Immunology, Inje University College of Medicine, Busan 47392, Republic of Korea; [b]Biomedical Research Center and Department of Biological Sciences, University of Ulsan, Ulsan 44610, Republic of Korea; [c]Department of Biochemistry, Inje University College of Medicine, Busan 47392, Republic of Korea; [d]Department of Hemato/Oncology, Busan Paik Hospital, Inje University College of Medicine, Busan 47392, Republic of Korea; [e]Advanced Research Center for Multiple Myeloma, Inje University College of Medicine, Busan 47392, Republic of Korea; [f]Department of Nephrology, Busan Paik Hospital, Inje University College of Medicine, Busan 614-735, Republic of Korea; [g]College of Pharmacy, Pusan National University, Busan 46241, Republic of Korea; and [h]Department of Hematology, Hokkaido University Graduate School of Medicine, Sapporo, Hokkaido 060-8638, Japan

Edited by John Dipersio, Washington University School of Medicine, and accepted by Editorial Board Member Carl F. Nathan June 5, 2017 (received for review September 12, 2016)

**The lung is a prototypic organ that was evolved to reduce immunopathology during the immune response to potentially hazardous endogenous and exogenous antigens. In this study, we show that donor CD4$^+$ T cells transiently induced expression of indoleamine 2,3-dioxygenase (IDO) in lung parenchyma in an IFN-γ–dependent manner early after allogeneic hematopoietic stem cell transplantation (HSCT). Abrogation of host IDO expression by deletion of the IDO gene or the IFN-γ gene in donor T cells or by FK506 treatment resulted in acute lethal pulmonary inflammation known as idiopathic pneumonia syndrome (IPS). Interestingly, IL-6 strongly induced IDO expression in an IFN-γ–independent manner when deacetylation of STAT3 was inhibited. Accordingly, a histone deacetylase inhibitor (HDACi) could reduce IPS in the state where IFN-γ expression was suppressed by FK506. Finally, L-kynurenine produced by lung epithelial cells and alveolar macrophages during IPS progression suppresses the inflammatory activities of lung epithelial cells and CD4$^+$ T cells through the aryl hydrocarbon receptor pathway. Taken together, our results reveal that IDO is a critical regulator of acute pulmonary inflammation and that regulation of IDO expression by HDACi may be a therapeutic approach for IPS after HSCT.**

acute lethal pulmonary inflammation | IFN-γ | Th2/Th17 cells | indoleamine 2,3-dioxygenase | aryl hydrocarbon receptor

Indoleamine 2,3-dioxygenase (IDO) is a rate-limiting enzyme of tryptophan catabolism along the kynurenine pathway. The immunosuppressive mechanism of IDO is mediated by depletion of tryptophan and/or the accumulation of catabolites collectively known as kynurenines (1–5). Recently, L-kynurenine, a product of IDO, has been identified as an endogenous ligand for the aryl hydrocarbon receptor (AhR), which is a ligand-activated transcription factor belonging to the steroid receptor family (6, 7). It is now clear that the IDO–AhR pathway contributes to immune homeostasis by promoting modulation of innate and adaptive immune responses. Whereas IFN-γ is the most prominent inducer of IDO in various cell types, IL-6 also can induce the enzyme expression in astrocytes and neuronal and cancer cells by stimulating the JAK/STAT3 signaling pathway (8, 9). By contrast, IL-6 has been implicated in the pathophysiology of Th17-mediated pulmonary inflammations such as idiopathic pulmonary syndrome (IPS) (10, 11). Thus, the IL-6–STAT3 pathway might be immunosuppressive or immunostimulatory in a context-dependent way.

The lung was evolved to develop tolerance mechanisms to avoid severe immunopathology during the immune response to pathogens (12, 13). High levels of IDO are expressed in the lung during microbial infections. IFNs seem to be required for IDO expression by microbial components (14, 15) and IDO expressed in epithelial cells prevents immunopathology mediated by Th cells after microbial infections (16). It is clear that defects in IDO expression in cystic fibrosis and granulomatous disease is associated with unchecked inflammation caused by infections (16, 17). However, the function of IDO in noninfectious acute pulmonary inflammation remains unclear.

A histone deacetylase inhibitor (HDACi) exhibits immunomodulatory activities as well as antitumor properties (18). In murine models of hematopoietic stem cell transplantation (HSCT), administration of suberanilohydroxamic acid (SAHA; vorinostat) ameliorates acute graft-versus-host disease (GVHD) by reducing proinflammatory cytokines (19). Subsequent studies show that HDACi-induced suppression of GVHD requires IDO expression in dendritic cells (DCs) (20). Clinical trials of HDACi have reported a decrease in acute GVHD (21). There are enhanced regulatory T cells (Tregs) in patients treated with SAHA (22), showing a positive relationship between these cells and HDACi-primed DCs. Interestingly, acetylation of STAT3 is critical for IDO expression (22, 23). However, which signal triggers STAT3 activation after HDACi treatment is not known in GVHD settings. In the present study, we provide evidence that IL-6 and HDACi are essential for IDO expression, which is protective from IPS. Clinically important, HDACi can inhibit IPS in the condition that IFN-γ expression is suppressed by a calcineurin inhibitor (CNI). This combination of

## Significance

Indoleamine 2,3-dioxygenase (IDO) is a rate-limiting enzyme in the metabolism of tryptophan and plays critical roles in immune regulation to avoid severe immunopathology. We demonstrate that IFN-γ signaling in lung parenchyma prevents idiopathic pneumonia syndrome by inducing IDO expression; inhibition of deacetylation of STAT3 potentiates IDO expression induced by IL-6 in an IFN-γ–independent manner; inhibition of IDO expression by immunosuppressants can be reversed by a histone deacetylase inhibitor; and finally, L-kynurenine acts on lung epithelial cells and CD4$^+$ T cells through the aryl hydrocarbon receptor to suppress their inflammatory activities. Our results indicate that proinflammatory IFN-γ and IL-6 expressed within a short time range early after pulmonary inflammation is indispensable in protecting the lung from devastating immunopathology.

Author contributions: S.-M.L., W.-S.L., T.T., B.K., and S.-K.S. designed research; S.-M.L. and H.Y.P. performed research; E.H.Y., J.K., S.-G.P., I.-W.C., I.C., S.-W.K., and H.Y. contributed new reagents/analytic tools; S.-M.L., H.Y.P., W.H.J., and S.-K.S. analyzed data; and S.-M.L., Y.-S.S., B.K., and S.-K.S. wrote the paper.

The authors declare no conflict of interest.

This article is a PNAS Direct Submission. J.D. is a guest editor invited by the Editorial Board.

Freely available online through the PNAS open access option.

[1]To whom correspondence should be addressed. Email: sseo@inje.ac.kr.

This article contains supporting information online at www.pnas.org/lookup/suppl/doi:10.1073/pnas.1615280114/-/DCSupplemental.

GVHD prophylaxis may be effective in preventing general GVHD, because IFN-γ is beneficiary for IPS, but harmful for intestinal GVHD.

## Results

**Differential Expression of IDO in GVHD Target Organs by Donor T-Cell–Derived IFN-γ.** Although the function of IDO has been demonstrated in intestinal GVHD (24, 25), its role in other GVHD target organs is unknown. Therefore, we initially examined the distribution of IDO expression in various GVHD target organs in three different allogeneic murine HSCT models. As previously described (24), IDO was strongly expressed in the colon at day 7 after HSCT. Interestingly, IDO expression was also notably observed in the lungs in all of the different models (Fig. 1*A*). However, the spleen and liver did not exhibit a visible increase in IDO expression. Quantitative real-time PCR analysis confirmed the differential expression patterns of IDO mRNA in these organs (Fig. 1*B*). To further characterize IDO expression in the lung, we performed immunohistochemistry (IHC) and flow cytometry analysis. IHC revealed that IDO staining was observed mainly in the epithelial layer (Fig. 1*C*) and we further confirmed the expression of IDO in epithelial cells identified with $EpCAM^+$ using flow cytometry (Fig. S1*A*). In addition to the identification of epithelial cells, the positive cells identified by IHC have been morphologically shown to be macrophages (Fig. 1*C*). Indeed, analysis of immunofluorescent staining confirmed colocalization of IDO in $EpCAM^+$ or $F4/80^+$ cells (Fig. 1*D*). According to a previous protocol, we used anti-F4/80 and anti-CD11c to identify lung interstitial macrophages (IMs), alveolar macrophages (AMs), and DCs (26). IDO was predominantly expressed in $F4/80^+CD11c^+$ AMs but not in the other cell types (Fig. S1*B*). These data indicate that IDO expression is prominently induced in the lung and colon after HSCT, and the sources of IDO expression in the lung are predominantly epithelial cells and AMs.

Donor T-cell–derived IFN-γ has been regarded as a principle inducer of IDO expression in colon tissue after HSCT (24). We next sought to determine whether IFN-γ of donor T cells induces IDO expression in the lungs of recipients after HSCT. In contrast to the recipients of WT T cells, IDO was not expressed in the lungs of the recipients of IFN-$\gamma^{-/-}$ T cells (Fig. 2*A*). Consistently, the absence of IDO was observed in the organ of the IFN-γ receptor$^{-/-}$ (IFN-γ$R^{-/-}$) that received WT donor T cells (Fig. 2*B*). We also confirmed that IDO expression was limited in the $H\text{-}2b^+$ $F4/80^+$ recipient cells using flow cytometry analysis (Fig. 2*C*), indicating that donor T-cell–derived IFN-γ induces expression of IDO in the lungs of recipients after HSCT.

We next determined the kinetics of IDO and IFN-γ in the lung after HSCT. At day 5 after HSCT, IDO was expressed. IDO expression peaked at day 7 and subsequently decreased (Fig. 2*D*). The kinetics of IFN-γ expression were similar to that of IDO (Fig. 2*E*). Levels of IDO in the colon surged at day 7, declined to a basal level by day 14, and continued to increase thereafter (Fig. S1*C*). IFN-γ showed a similar kinetics pattern of expression in the colon (Fig. S1*D*). Taken together, these data indicate that IDO is highly and transiently expressed at an early stage in the lung by donor T-cell–derived IFN-γ after HSCT.

**IDO$^{-/-}$ Recipient Mice Display Accelerated Mortality After HSCT.** After observing the induction of IDO expression in the lung after HSCT, we next investigated the effect of the enzyme activity on lung- and colon-specific GVHD. When GVHD was induced by a higher dose of donor T cells ($5 \times 10^6$ per mouse), IDO$^{-/-}$ recipients exhibited more rapid mortality and higher clinical scores compared with WT recipients (Fig. 3*A*). IDO$^{-/-}$ mice also had a markedly higher pathological score for lung GVHD at day 10 but WT and IDO$^{-/-}$ mice had an almost equal pathological score for intestinal GVHD (Fig. 3*B*). Induction of GVHD with a lower dose of donor T cells ($2 \times 10^6$ per mouse)

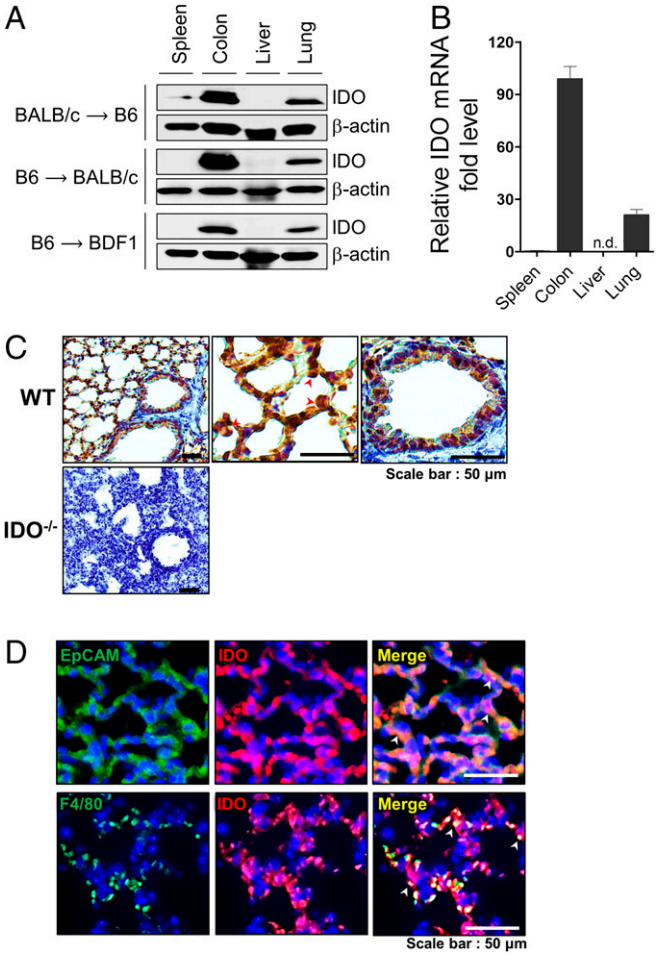


**Fig. 1.** IDO expression is predominantly induced in the lung and colon after HSCT. (*A*) The indicated lethally irradiated (950 cGy) recipient mice were injected with the indicated allogeneic donor T cells ($2 \times 10^6$) plus TCD-BM ($5 \times 10^6$). IDO protein expression was detected in the indicated organs from recipients on day 7 by Western blotting. One representative of four similar experiments is presented. (*B* and *C*) Lethally irradiated B6.WT or B6.IDO$^{-/-}$ recipients were injected with T cells ($2 \times 10^6$) plus TCD-BM ($5 \times 10^6$) from BALB/c. Organs were harvested at day 7 after HSCT. (*B*) IDO mRNA levels were determined by real-time PCR. The relative expression was presented as a fold change to the control group normalized to a fold value of 1. Lungs of naïve B6.WT mice were used as a control. The data are one of three independent experiments ($n$ = 9–10 per group). (*C*) Immunohistochemical staining of IDO in the lungs of recipients. Representative images of WT or IDO$^{-/-}$ recipients are presented. Magnification, 100× (*Left*) and 400× (*Middle* and *Right*). Arrows indicate cells that are morphologically macrophages. (*D*) Immunofluoresence staining of IDO and F4/80 or EpCAM. Blue, DAPI staining. Arrows indicate colocalization.

resulted in acute lethality in a minor number of IDO$^{-/-}$ recipients but a majority of mice had late-stage mortality over 50 d (Fig. S2*A*). Although the lung of IDO$^{-/-}$ recipients had a higher pathological score at day 35, its gap between the two groups was smaller compared with when GVHD was induced with a higher dose of donor T cells (Fig. 3*B* and Fig. S2*B*). By contrast, intestinal GVHD was more severe in IDO$^{-/-}$ recipients at this time (Fig. S2*B*). Altogether, our results seem to indicate that acute lethality in IDO$^{-/-}$ recipients might be associated with severe IPS in the former model, whereas late-stage mortality in the later model might be largely due to intestinal GVHD.

Th2 and Th17 cells have been revealed as the pathogenic cell type using murine IPS models (27–29). Indeed, expression of IL-4 and IL-17 was significantly increased with a different kinetic in the

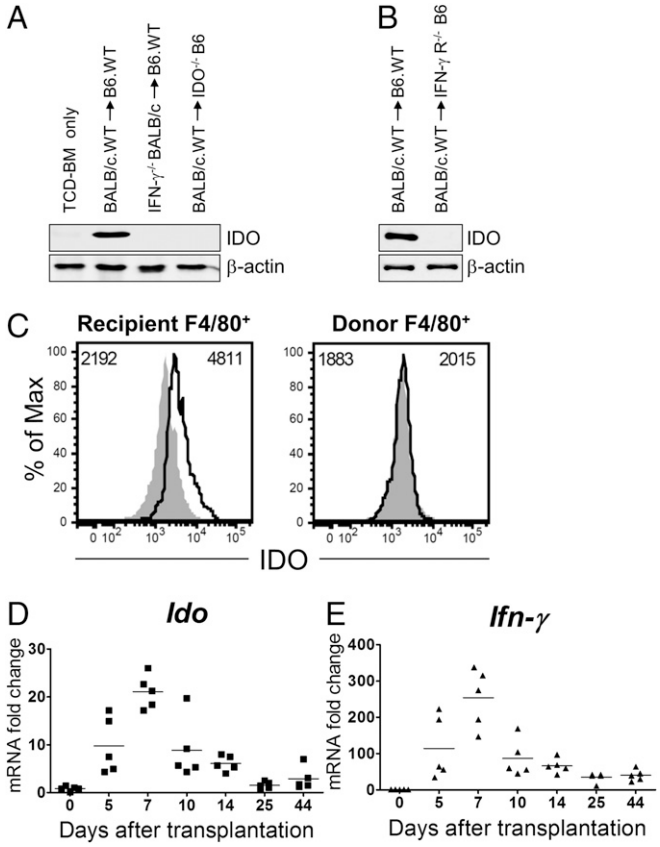


**Fig. 2.** Donor T-cell–derived IFN-γ transiently induces IDO expression in the lungs of recipients. Lethally irradiated (950 cGy) B6.WT, B6.IDO$^{-/-}$, or B6.IFN-γR$^{-/-}$ recipients were injected with BALB/c.WT ($2 \times 10^6$) or BALB/c.IFN-γ$^{-/-}$ T cells ($2 \times 10^6$) plus BALB/c.WT TCD-BM ($5 \times 10^6$). (*A* and *B*) IDO expression was detected in the lungs on day 7 by Western blotting. (*C*) Cells were isolated from the lungs of B6.WT or B6.IDO$^{-/-}$ recipients administered BALB/c T cells plus TCD-BM on day 7, stained with anti-H-2b, and then stained for intracellular IDO and analyzed by flow cytometry. Representative histograms for IDO expression in recipient (H-2b$^+$F4/80$^+$) and donor (H-2b$^-$F4/80$^+$) macrophages are presented. Open histograms, B6.WT; gray histograms, B6.IDO$^{-/-}$. (*D* and *E*) Kinetics of IDO (*D*) and IFN-γ (*E*) expression in the lungs were measured using real-time PCR at the indicated time points after transplantation. The relative expression was presented as a fold change to the control group (lungs of naïve B6.WT mice) normalized to a fold value of 1. The data are one of three independent experiments.

lung of IDO$^{-/-}$ recipients (Fig. 3*C*). IDO$^{-/-}$ mouse lungs also exhibited an increasing expression pattern of proinflammatory cytokines, TNF-α and IL-6, as GVHD progressed (Fig. 3*C*). However, expression of these cytokines was not so evident in the lungs of WT recipients (Fig. 3*C*). In addition, we observed that proliferating Ki67$^+$ and IL-4– and IL-17A–producing CD4$^+$ T cells were markedly increased in the lungs of IDO$^{-/-}$ recipients compared with WT recipients (Fig. 3 *D*–*F*). We confirmed severe IPS in IDO$^{-/-}$ recipients that received chemotherapy conditioning or different types of donors such as Bm12 (only a single MHC class II gene mismatched) or 129 (MHC matched but minor histocompatibility antigen mismatched) (Fig. S3).

Absence of IDO in the host did not affect the percentage of Tregs in the lung (Fig. S4*A*). Analysis of FoxP3, IL-10, and TGF-β mRNA in the lung showed no difference in their expression between WT and IDO$^{-/-}$ recipients (Fig. S4*B*). More importantly, depletion of donor Tregs did not deteriorate IPS or lung inflammation (Fig. S4 *C* and *D*). Taken together, our data indicate that induced IDO within the lung after HSCT effectively suppresses pathogenic Th2 and Th17 cell expansion in a Treg-independent manner, inhibiting IPS.

**IFN-γ Administration Reduces IPS Mediated by IFN-γ$^{-/-}$ Donor T Cells.** Recipients administered IFN-γ$^{-/-}$ donor T cells exhibit increased mortality compared with recipients administered WT donor T cells (27, 30). Therefore, we addressed whether the absence of IDO expression is associated with the lung damage of the recipient given IFN-γ$^{-/-}$ donor T cells. To test this hypothesis, we administered recombinant IFN-γ at days 5 and 7 after HSCT to induce IDO expression. Restoration of IDO expression was observed in the lungs of the recipients of IFN-γ$^{-/-}$ donor T cells by administering IFN-γ (Fig. 4 *A* and *B*). The mortality, the severe lung injury and the increased pathogenic cytokine levels in the lungs of the recipients administered IFN-γ$^{-/-}$ donor T cells were significantly decreased by IFN-γ treatment (Fig. 4 *C*–*E*). However, a treatment effect for IFN-γ was not observed in the IDO$^{-/-}$ recipients. We further confirmed the regulatory role of IFN-γ signaling in IPS using IFN-γR$^{-/-}$ recipients (Fig. S5). As shown previously (27, 30), IFN-γ$^{-/-}$ donor T cells induced mild intestinal GVHD in WT recipients (Fig. S6*A*). Injection of IFN-γ decreased the severity of intestinal GVHD in WT recipients of IFN-γ$^{-/-}$ donor T cells (Fig. S6*A*). In this case, exogenous IFN-γ induced expression of IDO in the intestine (Fig. S6*B*). IDO$^{-/-}$ recipient of IFN-γ$^{-/-}$ donor T cells displayed intestinal GVHD, as seen in WT recipients of WT donor T cells but injection of IFN-γ had no effect on intestinal GVHD severity (Fig. S6*A*), suggesting that there is an IFN-γ–independent pathogenic mechanism for intestinal GVHD in IDO$^{-/-}$ recipients.

**CNI Treatment Seems to Deteriorate IPS Through Inhibition of IDO Expression.** CNIs potently inhibit IFN-γ secretion from T cells (31, 32) and are most widely used in the clinic for pharmacological GVHD prophylaxis (33). We examined whether CNI treatment influences the development of IPS associated with the inhibition of IDO expression. Although general survival was statistically improved by FK506 treatment, we observed worse clinical GVHD scores in recipients of FK506 compared with recipients of the control treatment at an early stage (Fig. 5*A*). In FK506-treated recipients, we found that lung injury was increased compared with control mice (Fig. 5*B*). Furthermore, levels of pathogenic cytokines were increased in the lungs of FK506-treated recipients (Fig. 5*C*). In contrast, FK506 treatment suppressed both early- and late-stage intestinal GVHD (Fig. S6*C*). These data demonstrated that increased severity and lethality after FK506 treatment at an early period might be involved in IPS. Based on this observation, we further tested whether this lung injury effect of CNI was attributable to its ability to inhibit IDO expression through inhibition of IFN-γ production. In vivo administration of FK506 strongly inhibited expression of IDO in the lung (Fig. 5*D*) but infusion of IFN-γ in FK506-treated recipients restored its expression (Fig. 5*E*) and attenuated the lung injury (Fig. 5*F*). However, this effect of IFN-γ treatment was not observed in the IDO$^{-/-}$ recipients (Fig. 5*F*). These results demonstrated that treatment of FK506 contributes to IPS after HSCT and may be responsible for inhibiting IDO expression by inhibiting IFN-γ production.

**HDACi Induces IDO Expression in an IFN-γ–Independent Manner.** Although IFN-γ–mediated STAT1/IRF1 signaling is a critical intracellular pathway for IDO transcription, it has also been shown that enhancing STAT3 acetylation through HDAC inhibition can induce IDO expression in DCs (23). To determine whether HDACi is capable of inducing IDO expression via an IFN-γ–independent mechanism, we administered two pan-HDACis, SAHA and SB939 (pracinostat), to recipients of IFN-γ$^{-/-}$ donor T cells. In contrast to vehicle treatment, up-regulation of IDO and acetylated STAT3 was clearly observed in the lungs of recipients treated with these inhibitors (Fig. 6 *A* and *B*). Interestingly, peak levels of the IDO and acetylated STAT3 protein

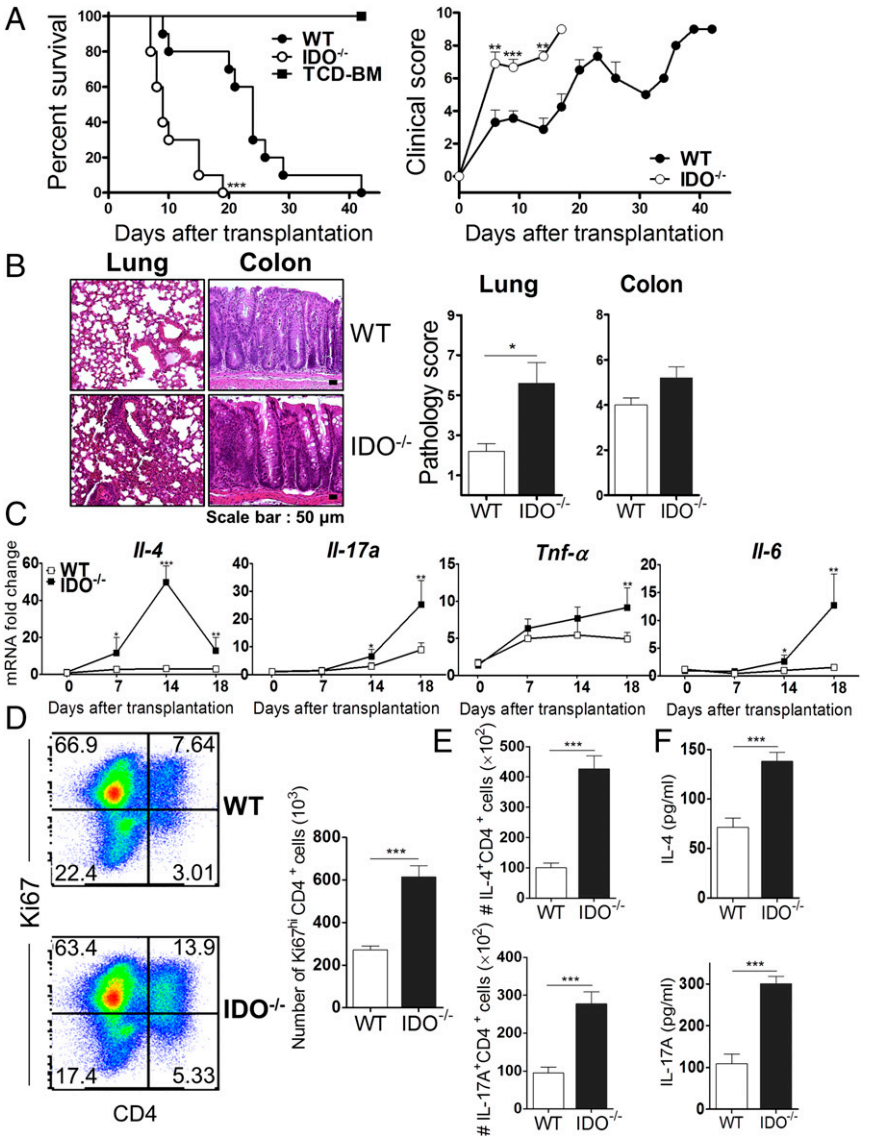


**Fig. 3.** Acceleration of mortality in IDO$^{-/-}$ recipient mice is associated with IPS. Lethally irradiated (950 cGy) B6.WT ($n = 10$) or B6.IDO$^{-/-}$ recipients ($n = 10$) were injected with T cells ($5 \times 10^6$) plus TCD-BM ($5 \times 10^6$) from BALB/c donors. (*A*, *Left* and *Right*) Survival and clinical GVHD scores, respectively. Representative data from one of two independent experiments are presented. (*B*) Lungs and colons were collected from each group of recipients on day 10 and stained with hematoxylin and eosin (H&E). Representative images (100×, *Left*) are shown. (*Right*) Histopathological scoring of the lung and colon. (*C*) Lungs were collected from each group of recipients at the indicated time points. Cytokine mRNA levels were determined by real-time PCR. The relative expression was presented as a fold change to the control group (lungs of naïve B6.WT mice) normalized to a fold value of 1. (*D*) Single-cell suspensions of lung tissue from each recipient were prepared on day 11 and stained for CD4 and Ki67 and then assessed using flow cytometry. Representative dot plots for Ki67$^+$CD4$^+$ T cells are presented (*Left* column). The graph summarizes the total number of Ki67$^+$CD4$^+$ T cells from WT ($n = 5$) and IDO$^{-/-}$ ($n = 5$) recipients (*Right* column). (*E* and *F*) Cells from the lungs of each recipient were stimulated with CD3/CD28 for 4 h (*E*) or 24 h (*F*). (*E*) Cells were stained for intracellular IL-4 or IL-17A and analyzed by flow cytometry. The graph summarizes the total number of IL-4$^+$CD4$^+$ or IL-17A$^+$CD4$^+$ T cells from WT ($n = 5$) and IDO$^{-/-}$ ($n = 5$) recipients. (*F*) IL-4 or IL-17A in cell culture supernatants. The data are one of three independent experiments. $^*P < 0.05$; $^{**}P < 0.01$; $^{***}P < 0.001$. The data represent the mean ± SEM.

in the lung were more remarkably increased after SB939 treatment compared with SAHA treatment. Using quantitative real-time PCR analysis, we confirmed that SB939 exhibited a more potent capacity to induce IDO expression in the absence of IFN-γ compared with SAHA (Fig. 6*C*). We next evaluated whether IPS induced by the lack of IFN-γ signaling can be prevented by the restoration of IDO expression by treatment with HDACi. Histopathology and survival data clearly revealed that treatment with SB939 in WT but not in IDO$^{-/-}$ mice prevented IPS (Fig. 6 *D* and *E*). Although SAHA treatment ameliorated IPS, it failed to decrease mortality. These results indicated that HDACi administration induced IDO in the lungs of recipients in the absence of IFN-γ signaling, which prevented IPS. Moreover, our data demonstrated that SB939 may have a stronger ability to induce IDO and a stronger functional activity than SAHA.

Next, we determined the mechanism of IDO induction by the administration of HDACi in our HSCT model. We observed induction of IDO and increased levels of acetyl-STAT3 in the lungs of recipients of IFN-γ$^{-/-}$ donor T cells after treatment with SB939 but not in those of recipients of T-cell–depleted bone marrow (TCD-BM) only (Fig. 7*A*). These data suggest that HDACi may require an unknown factor, which is secreted during strong lung inflammation, to acetylate STAT3 and subsequently induce IDO expression. To determine which factor contributes

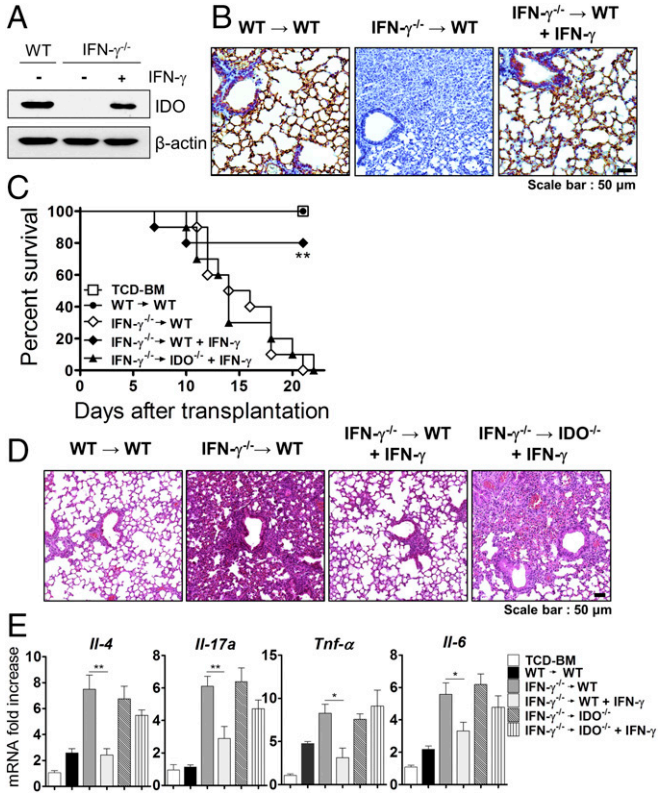


**Fig. 4.** IFN-$\gamma^{-/-}$ donor T-cell–mediated IPS is associated with the absence of IDO. Lethally irradiated (950 cGy) B6.WT ($n = 10$) or B6.IDO$^{-/-}$ ($n = 10$) recipients were injected with BALB/c.WT ($2 \times 10^6$) or BALB/c.IFN-$\gamma^{-/-}$ T cells ($2 \times 10^6$) plus BALB/c.WT TCD-BM ($1 \times 10^7$). Recipients were treated i.p. with IFN-γ on days 5 and 7 after transplantation. (*A* and *B*) IDO expression was detected in the lung on day 9 by Western blotting (*A*) and IHC (*B*). (*C*) Survival was monitored daily. The data are one of two independent experiments. (*D*) Lungs were collected from each group of recipient mice on day 9 and stained with H&E (100×). (*E*) Cytokine mRNA levels in the lungs were measured on day 9. The relative expression was presented as a fold change to the control group (lungs of TCD-BM only) normalized to a fold value of 1. The data are one of three independent experiments. $*P < 0.05$; $**P < 0.01$.

to the induction of STAT3 acetylation after treatment with SB939, we analyzed the cytokine environment in the lung because cytokines acetylate STAT3 via class I HDAC inhibitors (34). IL-6, TNF-α, and IL-1β levels were significantly increased in the lungs of recipients of IFN-$\gamma^{-/-}$ T cells compared with recipients of TCD-BM only (Fig. 7*B*). To identify the cytokine that contributes to the induction of IDO expression by HDACi, we performed in vitro experiments using the murine macrophage cell line RAW264.7. HDACi-induced IDO expression and STAT3 acetylation were dominant in the presence of IL-6 (Fig. 7*C*). We further confirmed that in vivo blockade of IL-6 signaling with anti-IL-6R antibody or gp130 inhibitor SC144 markedly reduced SB939-induced IDO expression and STAT3 acetylation in the lung (Fig. 7 *D* and *E* and Fig. S7) and subsequently suppressed lung injury and inflammation (Fig. S7).

We also examined whether HDACi treatment induced IDO expression in FK506-administered recipients. SB939 treatment in these mice restored IDO expression (Fig. 7*F*) and attenuated the lung injury, but these effects were not observed in FK506-treated IDO$^{-/-}$ mice (Fig. 7*G*). These data suggest that IDO expression should require sustained acetylation of STAT3 after its induction by IL-6 and that IDO in turn result in suppression of IL-6 expression. Taken together, these data suggest that CNI-induced IPS can be ameliorated by HDACi most likely via an IL-6–dependent mechanism.

**Induction of IDO Expression Prevents IPS via AhR.** IDO creates its antiinflammatory effects by metabolizing tryptophan into L-Kyn which binds and activates the immunomodulatory transcription factor AhR (6). We investigated whether AhR would be involved in the inhibitory effect of HDACi on IPS. Administration of SB939 resulted in markedly increased production of L-Kyn in the lung (Fig. 8*A*). An AhR-specific antagonist CH-223191 completely abolished the expression of CYP1B1, an AhR target gene, but not IDO mRNA (Fig. 8*B*), suggesting that SB939 may induce the expression of CYP1B1 transcription through the IDO–AhR axis. Importantly, CH-223191 abrogated SB939-induced suppression of lung injury and inflammation (Fig. 8 *C* and *D*). Administration of CH-223191 alone had no effect on GVHD survival and lung damage (Fig. 8*C* and Fig. S8). These results indicate that the inhibitory effect of HDACi on IPS may be mediated by the IDO–AhR signaling pathway.

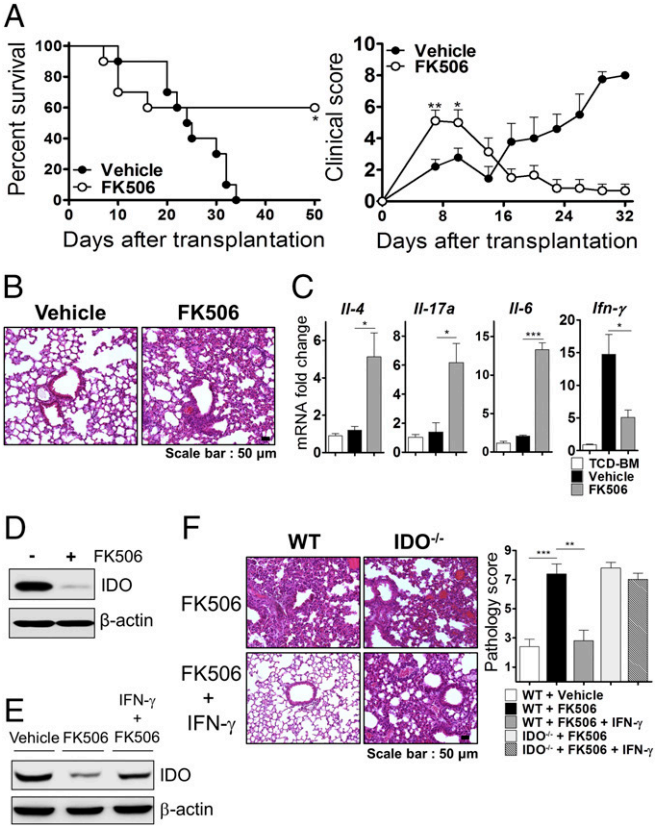


**Fig. 5.** CNI treatment seems to cause IPS by blocking IDO induction. Lethally irradiated (950 cGy) B6 recipients were injected with TCD-BM ($5 \times 10^6$) plus T cells ($5 \times 10^6$) from a BALB/c donor and were given FK506 (15 mg/kg) i.p. once daily from day 0 to day 9. (*A*, *Left* and *Right*) Survival and clinical GVHD scores, respectively. The data are one of two independent experiments. (*B*) Lung tissue was collected from each group of recipient mice on day 9 and stained with H&E (100×). (*C*) Cytokine mRNA levels in the lung were measured on day 9. The relative expression was presented as a fold change to the control group (lungs of TCD-BM only) normalized to a fold value of 1. (*D*) IDO expression was detected in the lung on day 7 by Western blotting. (*E* and *F*) Recipients administered FK506 were treated with or without recombinant IFN-γ at 5 and 7 d after transplantation. (*E*) IDO expression was detected in the lung on day 9. (*F*) Representative images (100×, *Left*) and graphs of histopathological scoring (*Right*) of the lung on day 9 are presented. The data are one of three independent experiments. $*P < 0.05$; $**P < 0.01$; $***P < 0.001$.

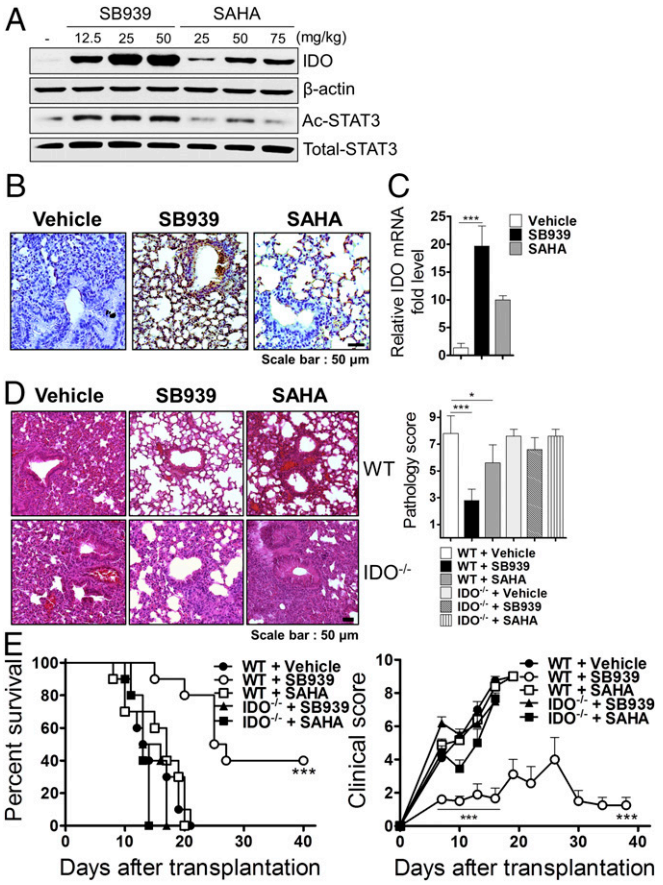


**Fig. 6.** Treatment of HDACi induces IDO in the absence of IFN-γ. (*A–D*) Lethally irradiated (850 cGy) B6.WT ($n = 10$) or B6.IDO$^{-/-}$ ($n = 10$) recipients were injected with BALB/c.IFN-γ$^{-/-}$ T cells ($1 \times 10^6$) plus BALB/c.WT TCD-BM ($5 \times 10^6$). (*A*) The recipients were treated with the indicated concentrations of the drugs i.p. once daily from day 0 to day 9. (*B* and *C*) The recipients were treated with SB939 (25 mg/kg) or SAHA (50 mg/kg). IDO and acetylated STAT3 (Ac-STAT3) was detected in the lung by Western blotting on day 9 (*A*), IHC (200×) (*B*), and real-time PCR (*C*). The data are one of three independent experiments. (*D*) Representative images (100×, *Left*) and graphs of histopathological scoring (*Right*) of the lung on day 9 are presented. (*E*) Lethally irradiated (950 cGy) B6.WT ($n = 10$) or B6.IDO$^{-/-}$ ($n = 10$) recipients were injected with BALB/c.IFN-γ$^{-/-}$ T cells ($2 \times 10^6$) plus BALB/c.WT TCD-BM ($1 \times 10^7$). The recipients were treated with SAHA (50 mg/kg) or SB939 (25 mg/kg) i.p. once daily from day 0 to day 17. (*Left* and *Right*) Survival and clinical GVHD scores, respectively. The data are one of two independent experiments. *$P < 0.05$; ***$P < 0.001$.

There was a marked decrease in CYP1B1 expression in the lung and intestine of IDO$^{-/-}$ recipients after HSCT (Fig. S9), confirming that production of L-Kyn is required for triggering the AhR signaling. We next wanted to investigate how the IDO–AhR pathway controls IPS. High levels of AhR expression were dominantly detected in CD4$^+$ T cells and epithelial cells in the lung on 7 d after HSCT (Fig. 9*A*). IFN-γ induced expression of IDO mRNA and consequent production of L-Kyn in primary lung epithelial cells (Fig. 9*B*). IFN-γ also induced CYP1B1 mRNA expression in an IDO-dependent manner (Fig. 9*B*). These results indicate that L-Kyn of epithelial cells and macrophages exerts its biological actions in response to cytokines in autocrine and paracrine ways. Consistent with this interpretation, we showed that L-Kyn blocked IL-1β–induced IL-6 expression in A549 lung epithelial cells but CH-223191 completely recovered IL-6 production (Fig. 9*C*). Knockdown of the AhR gene also abolished the suppressive effect of L-Kyn on IL-6 production induced by IL-1β (Fig. 9*D*).

To examine AhR signaling in CD4$^+$ T cells, we isolated AhR-expressing CD4$^+$ T cells from the 7-d lungs of IDO$^{-/-}$ recipients. Treatment with L-Kyn suppressed proliferation of polyclonally activated CD4$^+$ T cells (Fig. 9*E*) and their production of IL-4 and IL-17 (Fig. 9*F*). There was increased expression of CYP1B1 mRNA in CD4$^+$ T cells in response to L-Kyn (Fig. 9*G*). Taken together, our data suggest that L-Kyn produced by lung epithelial cells and alveolar macrophages suppresses IPS mainly through its action on lung epithelial cells and CD4$^+$ T cells.

## Discussion

Previously, Burman et al. investigated the relevance of IDO in the prevention of IPS via IFN-γ signaling in lung parenchymal cells (30). Using real-time PCR analysis from lung tissue after transplantation, the study demonstrated a 10-fold increase in IDO expression in WT recipients compared with IFN-γR$^{-/-}$ recipients. However, the inhibition of IDO activity in WT recipients using 1-methyl-tryptophan (1-MT) during HSCT did not result in the development of IPS. Thus, the study excluded the relevance of IDO in the prevention of IPS. Mauermann et al. also reported no IDO

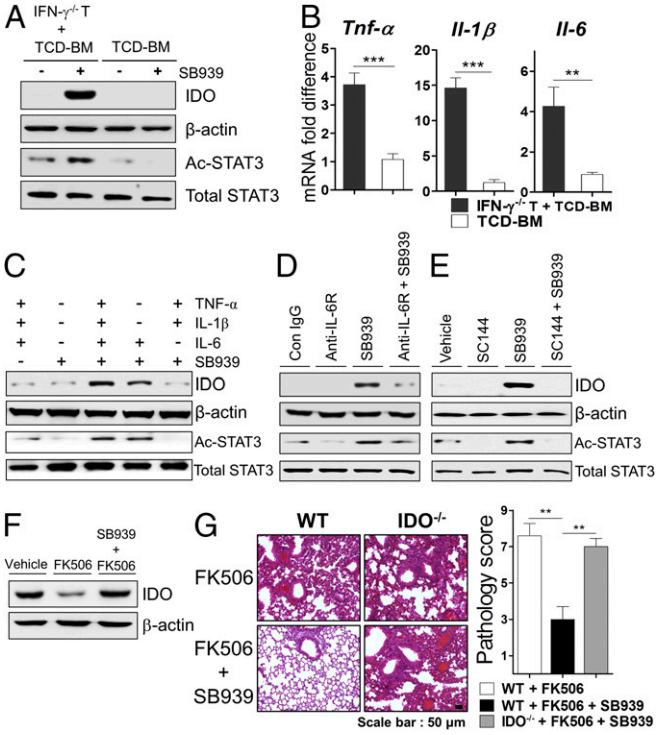


**Fig. 7.** IL-6 signaling is required for HDACi-induced IDO expression. (*A*, *B*, *D*, and *E*) Lethally irradiated (850 cGy) B6.WT recipients were injected with BALB/c TCD-BM ($5 \times 10^6$) with or without BALB/c.IFN-γ$^{-/-}$ T cells ($1 \times 10^6$). The recipients were treated with SB939 i.p. once daily from day 0 to day 9. (*A*) IDO and Ac-STAT3 were detected in the lung on day 9. (*B*) Cytokine mRNA levels in the lungs were measured on day 9. The relative expression was presented as a fold change to the control group (lungs of TCD-BM only) normalized to a fold value of 1. (*C*) RAW264.7 cells were treated with SB939 (0.5 μM) in the presence or absence of TNF-α (20 ng/mL), IL-1b (2.5 ng/mL), or IL-6 (10 ng/mL). IDO and Ac-STAT3 were detected by Western blotting. (*D* and *E*) The recipients were treated with anti–IL-6R mAb on days 3, 5, and 9 (*D*) or with SC144 every day from day 0 to day 9 (*E*). IDO and Ac-STAT3 were detected in the lung on day 9. (*F* and *G*) Lethally irradiated (950 cGy) B6 recipients were injected with TCD-BM ($5 \times 10^6$) plus T cells ($5 \times 10^6$) from BALB/c donors. Recipients were administered FK506 as in Fig. 6 and were treated with or without 25 mg/kg SB939 i.p. once daily from day 0 to day 9. (*F*) IDO was detected in the lung on day 9. (*G*) Representative images (100×, *Left*) and graphs of histopathological scoring (*Right*) of the lung on day 9 are shown. The data are one of three independent experiments. **$P < 0.01$; ***$P < 0.001$.

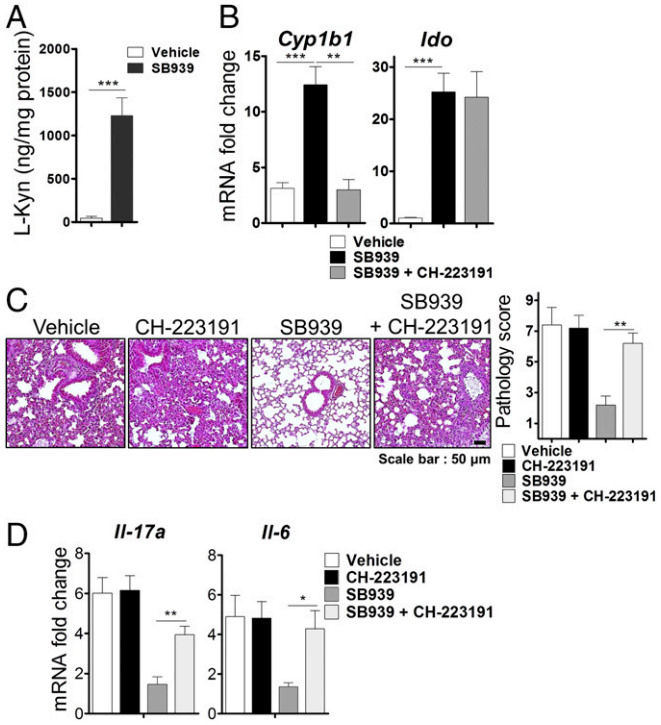


**Fig. 8.** HDACi-induced IDO expression prevents IPS via the AhR pathway. (*A–D*) Lethally irradiated (850 cGy) B6.WT recipients were injected with BALB/c TCD-BM ($5 \times 10^6$) with BALB/c.IFN-$\gamma^{-/-}$ T cells ($1 \times 10^6$). Recipients received SB939 (as in Fig. 7) and 10 mg/kg CH-223191 once daily from day 4 to day 8. Levels of L-Kyn (*A*) and IDO and CYP1B1 mRNA (*B*) in the lung were measured using ELISA and real-time PCR on day 9. (*C*) Representative images (100×, *Left*) and graphs of histopathological scoring (*Right*) of the lung on day 9. (*D*) Levels of cytokine mRNA in the lung were measured using real-time PCR on day 9. The relative expression was presented as a fold change to the control group (lungs of TCD-BM only) normalized to a fold value of 1. The data are one of three independent experiments. $*P < 0.05$; $**P < 0.01$; $***P < 0.001$.

mRNA expression after transfer of IFN-$\gamma^{-/-}$ $CD4^+$ T cells, whereas IDO mRNA was present after transfer of WT $CD4^+$ T cells (28). In the present study, we observed clear expression of IDO protein in the lungs of recipients at 5–14 d after HSCT. In addition, severe lung injury was associated with higher lethality in IDO$^{-/-}$ recipients. The cause of the discrepancy between our data and Burman et al.'s data are not known but may be due to the difference in the levels of IDO in the lung depending on the experimental model used. Burman et al. (30) used granulocyte colony-stimulating factor (G-CSF)–mobilized donor splenocytes as a donor graft that exhibits relatively less IFN-γ production compared with a donor graft with isolated normal naïve T cells plus TCD-BM (35). IDO and IFN-γ levels in the lung tissue were considerably reduced in the G-CSF–mobilized donor grafts used by Burman et al. (30) compared with our HSCT model (Fig. S10). Levels of IFN-γ might not reach the threshold required for IDO up-regulation in their study. Additionally, the chemical inhibition of IDO by 1-MT is by far less efficient than genotypic deletion used in the present study. Thus, our data indicate that the protective activity of IDO on IPS correlates with the levels of IDO expression (36).

IDO is induced in various types of cells; however, it has a different mechanism of suppression depending upon cell type. IDO expression in antigen-presenting cells (APCs) such as DCs and macrophages contributes to peripheral immune tolerance by inhibiting T-cell expansion and inducing Treg responses (37–39). However, IDO expression in nonimmune cell types, such as epithelial cells, can inhibit immune effector processes in local tissues to limit collateral damage (14, 15). Our data indicate that IDO expression was mainly detected in the host lung epithelial cells and AMs rather than in DCs, which effectively inhibited the expansion of inflammatory T cells within the lung. However, Treg responses were not altered. These results demonstrate that IDO activity may inhibit local inflammatory responses but may not result in tolerance induction. IDO activity might be associated with epithelial cells, which mainly account for all of the IDO activity in the lung (14), and these cells are the major cell type that responds to IFN-γ and is protective against IPS (28, 30). Interestingly, IDO of epithelial cells seems to suppress inflammation at least partially by inhibiting their own ability to produce IL-6, through the L-Kyn–AhR axis, in response to a proinflammatory cytokine such as IL-1β (Fig. 9 *C* and *D*). Thus, epithelial cells are likely to have a self-regulating system for inflammation. In addition, L-Kyn produced by epithelial cells and probably by AMs appears to inhibit the activities of pathogenic $CD4^+$ T cells (Fig. 9 *E* and *F*). Because IDO expression in the lung was high and transient in the early phase of lung diseases (ref. 14 and Fig. 2*D*), the L-Kyn–AhR pathway seems to be critical in inhibiting early immune effector processes rather than tolerance induction. However, it is also possible to regulate the inflammatory T-cell–Treg balance through sustained IDO expression in AMs (40). Further studies are needed to dissect the contribution of epithelial cells and AMs as a cellular source of IDO to protect against IPS.

In the clinic, CNI-based immune suppression is used as a standard protocol for GVHD prophylaxis (33). Classically, CNIs down-regulate IL-2 synthesis, which prevents Th1 and CD8 T-cell functions and IFN-γ synthesis (31, 32). By contrast, cyclosphorin A (CsA) treatment promotes Th17 and Th2 responses after experimental lung transplantation and subsequently increases bronchiolitis obliterans (41). A more recent study demonstrated that CsA treatment preferentially expands alloantigen-specific Th17 cells within the lung by promoting lung parenchyma-derived IL-6, which promotes IPS (11). Therefore, we investigated whether CNI-induced IPS was associated with the regulation of IDO activity. Our results demonstrated that CNI exacerbates IPS by suppressing IDO expression as a result of down-regulation of IFN-γ production. Taken together, the study of Varelias et al. (11) and ours suggest that down-regulation of IFN-γ may cause dysregulated IL-6 and subsequent Th17 differentiation through inhibition of IDO expression.

IDO function in GVHD was initially demonstrated by Blazar and colleagues (24). They observed increased mortality in IDO$^{-/-}$ mice. A higher pathological score for colon GVHD and heavier T-cell infiltration to the colon at day 27 after HSCT were associated with increased mortality in IDO$^{-/-}$ mice. Consistently, our results demonstrated that late-stage mortality seemed to be associated with severe intestinal GVHD in IDO$^{-/-}$ mice (Fig. S2). Although Blazar and colleagues (24) did not investigate the cause of acute lethality observed in a small number of mice observed in their experiments, our data suggest that acute lethality may be due to severe IPS in IDO$^{-/-}$ recipients. Further studies will be warranted to reveal the causal relationship of IPS and intestinal GVHD with mortality after HSCT transplantation.

Interestingly, 10 consecutive injections of FK506 induced acute lethality in 40% mice but the rest of the mice survived until termination of the experiments (Fig. 5*A*). Early mortality in these mice seemed to be caused by severe IPS (Fig. 5*B* and Fig. S6*C*). Once FK506 administration was stopped, however, a majority of the mice that survived appeared to recover from IPS to some extent (Fig. S6*C*). FK506 treatment suppressed both early- and late-stage intestinal GVHD (Fig. S6*C*). As a matter of fact, our results from kinetics studies of IFN-γ expression (Fig. 2*E* and Fig. S1*D*) predicted these observations, because IFN-γ acted on both the lung and colon early after HSCT but predominantly on the colon when intestinal GVHD was fulminant late after HSCT. Our findings of

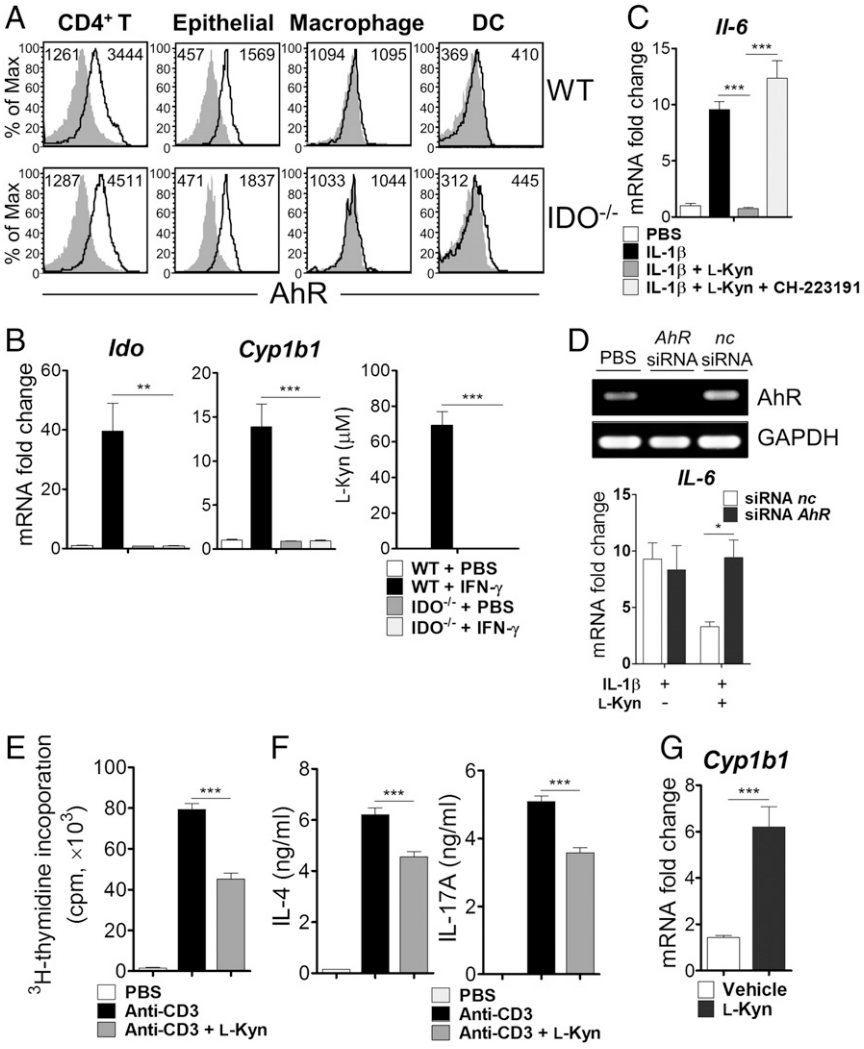


**Fig. 9.** Inhibition of the activities of epithelial cells and CD4$^+$ T cells by the L-Kyn–AhR axis. (*A*) Cells were isolated on day 7 from the lungs of B6.WT ($n = 4$) or B6.IDO$^{-/-}$ ($n = 4$) recipients of BALB/c T cells ($5 \times 10^6$) plus TCD-BM ($5 \times 10^6$) and stained for intracellular AhR. Representative histograms for AhR expression in CD4$^+$ T cells. Epithelial cells, macrophages, and DCs are presented. Gray histograms, isotype control staining; open histograms, anti-AhR staining. (*B*) Alveolar epithelial cells (AECs) were isolated from WT or IDO$^{-/-}$ mice and treated with recombinant IFN-γ. Levels of IDO and CYP1B1 mRNA were measured at 72 h after treatment with or without IFN-γ (200 units/mL) plus L-tryptophan (500 μM). The relative expression was presented as a fold change to the control group (untreated WT AECs) normalized to a fold value of 1. L-Kyn was measured by ELISA. (*C*) A549 cells were stimulated with IL-1β (12.5 ng/mL) after a 48-h pretreatment with or without L-Kyn (300 μM) or L-Kyn plus CH-223191 (10 μM). Levels of IL-6 mRNA were measured at 24 h after IL-1β treatment using real-time PCR. (*D*) A549 cells were transfected with AhR siRNA or control (*nc*) siRNA and levels of AhR mRNA was analyzed using RT-PCR (*Upper* column). Levels of IL-6 mRNA were analyzed as described above (*Lower*). The relative expression was presented as a fold change to the control group (PBS-treated A549) normalized to a fold value of 1. (*E–G*) CD4$^+$ T cells were isolated on day 7 from the lungs of B6.IDO$^{-/-}$ recipients of BALB/c T cells plus TCD-BM. (*E*) Isolated CD4$^+$ T cells were stimulated with anti-CD3 for 3 d in the presence or absence of L-Kyn. Cell proliferation was measured using [$^3$H]-thymidine incorporation. (*F*) Cytokines in cell culture supernatants. (*G*) Isolated CD4$^+$ T cells were treated with L-Kyn in the presence of IL-2. Levels of CYP1B1 mRNA were measured at 72 h after L-Kyn treatment. The relative expression was presented as a fold change to the control group (vehicle-treated T cells) normalized to a fold value of 1. The data are one of two independent experiments. $^{**}P < 0.01$; $^{***}P < 0.001$.

the deteriorating effect of FK506 on early IPS in our preclinical animal models may raise an issue for evaluating a general effect of immunosuppressants on early IPS in the clinic.

In this study, we found that administration of an HDACi potently induces IDO expression in the lungs of HSCT recipients in an IFN-γ–independent manner, resulting in the prevention of IPS. As clinical trials for HDACi that prevent acute GVHD are currently underway (21, 22), our findings may have clinical implications. In this study, the pan-HDAC inhibitor SB939 was identified as a potential inducer of IDO expression and thus an inhibitor of IPS. In comparison with SAHA, SB939 appeared to exhibit a stronger ability to induce IDO expression both in vivo and in vitro. Consequently, the inhibitory effects of SB939 on IPS were significantly increased compared with SAHA. SB939 is a new orally active hydroxamate-based HDACi that is currently in phase II clinical trials and that potently inhibits class I, II, and IV HDACs with excellent pharmacokinetic properties (42, 43). Compared with SAHA, SB939 exhibits increased oral bioavailability and half-life. In cancer models, SB939 accumulates in tumor tissue and induces sustainable inhibition of histone acetylation, which results in more enhanced antitumor efficacy than SAHA (42). Because SB939 induces sustainable inhibition of HDAC activity, it may induce IDO more strongly than SAHA through the accumulation of acetylated STAT3 in the lung tissue. Our results suggest that SB939 might be a candidate HDACi for the prevention of IPS.

STAT3 acetylation has been identified as the mechanism of HDACi-induced IDO expression (23). Our data demonstrated that IL-6 signaling is required for the accumulation of acetyl-STAT3 by HDACi, which results in the induction of IDO expression. In response to cytokine treatment, STAT3 protein is activated via acetylation on a single lysine residue by histone acetyltransferase p300 and via phosphorylation (34). The cytosolic acetylation of STAT3 results in protein dimerization and subsequent nuclear translocation followed by cytokine-stimulated DNA binding and transcriptional regulation. Because cytokine-mediated STAT3 acetylation is reversible by type I HDACs, STAT3 acetylation is strongly increased by the inhibition of HDACs. Therefore, IL-6 can create a microenvironment suitable for IDO induction by HDACi treatment. Because dysregulated IL-6 is a major mediator of IPS by driving on Th17 differentiation (11), IL-6 seems to have a self-regulating mechanism of shutting down its own expression via the IDO–AhR pathway (Fig. 9 *C* and *D*). It is interesting that IL-6 is required for the conversion of a pathogenic microenvironment into a tolerogenic microenvironment through functional IDO induction in the lung. Like IFN-γ, IL-6 may have a proinflammatory or antiinflammatory function depending upon conditions such as timing and quantity of its production during immune responses. Collectively, our results suggest that the inhibition of HDAC could provide clinically feasible strategies for preventing IPS in a CNI-based clinical setting.

In summary, the results of the present study suggest that the induction of IDO expression occurs in host lung parenchyma of HSCT recipients in an IFN-γ–dependent or –independent manner. More importantly, HDACi derepresses the blockade of IDO induction by decreasing IFN-γ and increasing IL-6. Therefore, the addition of HDACis, such as SB939, in the immunosuppressive protocol might be a suitable therapeutic strategy for the prevention and treatment of IPS.

## Materials and Methods

**Mice.** Female C57BL/6 (referred to as B6.WT herein; H-$2^b$), BALB/c (H-$2^d$), and B6D2F1 (H-$2^{b/d}$) mice were purchased from Charles River. B6.IDO$^{-/-}$ (H-$2^b$), BALB/c.IFN-γ$^{-/-}$ (H-$2^d$), and B6.IFN-γ receptor $^{-/-}$ (H-$2^b$) mice were purchased from The Jackson Laboratory. All of the mice were used at 8–12 wk of age. All of the animal procedures received the approval of the Institutional Animal Care and Use Committee at Inje University College of Medicine.

**HSCT.** B6.WT, B6.IDO$^{-/-}$, or B6.IFN-γ receptor $^{-/-}$ mice were exposed to two separate doses of total body irradiation (TBI) (850–950 cGy, $^{137}$Cs source at 108 rad/min) within 3 h to minimize the degree of gastrointestinal toxicity. Donor T cells were purified by AutoMACS-positive selection with anti-CD90 magnetic beads (Miltenyi Biotec) from total splenocytes of BALB/c.WT or BALB/c.IFN-γ$^{-/-}$ mice. TCD-BM was prepared from the tibia and femur of B6.WT mice. Recipients of TCD-BM were transplanted with or without purified T cells via a tail vein injection. All recipient mice received antibiotic (neomycin sulfate 25 μg/mL and polymyxin B sulfate 0.3 units/mL)-containing water for the first 2 wk after HSCT. Mice were monitored daily for survival and clinical score. The clinical score was based on weight loss, posture, activity, fur texture, and skin integrity as previously described (44).

**In Vivo Treatment.** Recipients were administered recombinant murine IFN-γ (100,000 units) i.p. (0.2 mL) on days 5 and 7 after transplantation. FK506 (InvivoGen) was dissolved in Cremophor EL and ethanol (1:1) and brought to a final concentration of 1.5 mg/mL in PBS. Recipients were administered 15 mg/kg FK506 i.p. (0.2 mL) once daily from day 0 to day 9. Administration of anti–IL-6R mAb (15A7; BioXcell) was performed as previously described (45). SAHA (Selleckchem) was dissolved first in DMSO and then diluted with distilled water (fourfold, vol/vol). SB939 (Selleckchem), CH-223191 (Sigma-Aldrich), or SC144 (Tocris) were dissolved in Cremophor EL and ethanol (1:1) and brought to a final concentration of 2.5 mg/mL, 1 mg/mL, or 0.4 mg/mL in PBS. Recipients were administered 50 mg/kg SAHA, 25 mg/kg SB939, or 4 mg/kg SC144 i.p. once daily from day 0 to day 9 or 17. Administration of CH-223191 (10 mg/kg) was performed as previously described (46).

**Histologic Analysis.** Lung and colon tissues were fixed in 10% formalin solution (Sigma-Aldrich) and embedded in paraffin. Paraffin-embedded tissues were cut into 5-μm sections and stained with H&E. Histopathologic scoring for lung was performed as previously described (47). For immunohistochemical analyses, antigens were unmasked by boiling tissue sections in citrate buffer (Vector Labs). Purified rabbit anti-mouse IDO (Enzo Life Science) for overnight at 4 °C, followed by subsequent steps as per manufacturer's instruction (Vectastain; Vector Labs). Positive staining was accomplished using DAB chromogenic substrate. Sections were counterstained with hematoxylin. Tissue morphology was assessed using a NanoZoomer 2.0 RS (Hamamatsu). For immunofluorescent staining, tissue sections were incubated with purified rabbit anti-mouse IDO plus purified rat anti-mouse F4/80 (Thermo Fisher Scientific) or purified mouse anti-mouse Cytokeratin (Thermo Fisher Scientific) Ab for overnight at 4 °C, followed by Alexa 594-conjugated goat anti-rabbit Ab (Molecular Probes) plus Alexa 488-conjugated goat anti-rat Ab (Molecular Probes) or Alexa 488-conjugated goat anti-mouse Ab (Molecular Probes). Sections were then counterstained with DAPI (Invitrogen). Images were captured using Olympus BX51 Microscope (Olympus) and pictures were analyzed using MetaMorph software (Molecular Devices).

**Western Blot Analysis.** Tissues were collected from recipients and immediately frozen on dry ice and kept at –80 °C until use. RAW264.7 cells ($1 \times 10^6$ cells per 3 mL) were pretreated with recombinant TNF-α (20 ng/mL), IL-1b (2.5 ng/mL), or IL-6 (10 ng/mL) in a 60-mm culture dish (Corning Costar) for 20 h. Cells were treated once daily with SB939 (0.5 μM) for 3 d. Western blot analysis was performed using either anti-IDO (1:2,000; Enzo Life Science), anti-STAT3 (1:1,000; Cell Signaling Technology), anti–acetyl-STAT3 (1:1,000; Cell Signaling Technology), or anti–β-actin (1:1,000; Cell Signaling Technology). Images were captured using LAS3000 (Fujifilm).

**Quantitative Real-Time PCR.** Total RNA was isolated from tissues or cells using TRIzol reagent (Invitrogen) according to the manufacturer's protocol. Four micrograms of total RNA was used to synthesize cDNA using a SuperScript III Kit (Invitrogen). PCR primers were designed using Massachusetts General Hospital (MGH) PrimerBank (https://pga.mgh.harvard.edu/primerbank). Real-time PCR was performed using iQ SYBR-Green Supermix on the iCycler iQ Detection System (Bio-Rad) according to the manufacturer's instructions. Relative gene expression levels were calculated using GAPDH as a control, where Ct (45 cycles) is the threshold cycle value.

**Flow Cytometry.** The following antibodies were purchased from eBioscience for flow cytometry: fluorescein isothiocyanate (FITC)-conjugated antibodies against IL-4 (BVD6-24G2), IL-17A (eBio17B7), F4/80 (BM8), and IgG2a isotype control; phycoerythrin (PE)-conjugated antibodies against EpCAM (G8.8), CD11c (N418), and isotype control; PE-Cy7–conjugated anti-CD4 (GK1.5) and isotype control; Alexa-Fluor 647-conjugated anti-Ki67 (SolA15) and isotype control; eFluor 660-conjugated anti-IDO (mIDO-48) and isotype control; eFluor 660-conjugated anti-AhR (4MEJJ) and isotype control; and purified anti-CD16/32 (2.4G2). To analyze IDO expression, lung tissues from perfused mice were chopped into small pieces and incubated with collagenase type IV (2.4 mg/mL; Sigma-Aldrich) for 1 h at 37 °C. Subsequently, cell fractions were harvested using a 30% Percoll gradient. Single-cell suspensions were obtained using a cell strainer (BD Falcon). Cells were incubated with 2.4G2 for 10 min at 4 °C and stained with antibodies against F4/80, EpCAM, CD11c, or CD4. The cells were washed and resuspended in a Cytofix/Cytoperm solution, and intracellular staining using anti-IDO or anti-AhR was performed according to the manufacturer's protocol. Fluorescence was measured using the FACSCanto II flow cytometer (BD Biosciences), and data were analyzed using FlowJo 9.6.4 software (Treestar). For cytokine staining, splenocytes ($2 \times 10^6$ cells per milliliter) were stimulated with plate-bound anti-CD3 (1.0 μg/mL, 145.2C11) and soluble anti-CD28 (0.5 μg/mL, 37.51) in the presence of GolgiPlug (BD Biosciences) in a 96-well plate (Corning Costar) at 37 °C for 4 h before staining.

**Cytokine Measurement.** Concentrations of IL-4 and IL-17A in cell culture supernatants were determined using the mouse Flex-Set cytokine bead array (BD Biosciences). All of the assays were performed according to the manufacturer's protocol.

**Measurement of L-Kynurenine.** Preparation of tissue homogenates were performed as previously described (14). L-Kyn concentration in tissue homogenates or cell culture supernatants was measured using the L-Kyn ELISA kit (ImmuSmol). ELISA was performed according to the manufacturer's protocol.

**Effects of L-Kyn Treatment.** A549 cells were transfected with AhR siRNAs or control siRNAs (Thermo Fisher Scientific) using Lipofectamine 2000 reagent (Invitrogen) at 37 °C for 120 h according to the manufacturer's protocol. Transfected cells ($1 \times 10^6$ cells per 3 mL) were stimulated with IL-1β (12.5 ng/mL) after a 48-h pretreatment with or without L-Kyn (300 μM) plus CH-223191 (10 μM) in a 60-mm dish (Corning Costar) at 37 °C for 72 h. To test the effects of L-Kyn on T cells, lung tissues from perfused mice were chopped into small pieces and incubated with collagenase type IV (2.4 mg/mL; Sigma-Aldrich) for 1 h at 37 °C. Cell fractions then were harvested using a 30% Percoll gradient. $CD4^+$ T cells were purified by AutoMACS-positive selection with anti-CD4 (L3T4) magnetic beads. Purified $CD4^+$ T cells ($1.5 \times 10^6$ cells per milliliter) were treated with soluble anti-CD3 (3 μg/mL) or recombinant human IL-2 (20 ng/mL; R&D Systems) with or without L-Kyn (300 μM) in a 96-well plate (Corning Costar) at 37 °C for 72 h. During the final 15∼17 h, the cells were pulsed with [$^3$H]-thymidine (1 μCi per well; Amersham Pharmacia), followed by collection on glass fiber filters and measurement of incorporated [$^3$H]-thymidine in 1450 MicroBeta Trilux Liquid Scintillation/Beta Counter (Wallac).

**Isolation of Alveolar Epithelial Cells.** Primary alveolar epithelial cells were isolated as previously described (48). In brief, dispase (Gibco-Invitrogen) was instilled into lung tissues of C57BL/6 mice via the trachea. The lungs were removed and incubated in a dispase-containing solution for 45 min at room temperature. The parenchymal tissue was carefully teased apart, and the cell suspension treated with DNase I (Sigma-Aldrich). Single-cell suspensions were obtained using a 70- and 40-μm cell strainer (BD Falcon). Alveolar epithelial cells were isolated by AutoMACS-negative selection with anti-CD45 and anti-CD146 magnetic beads (Miltenyi Biotec). The $CD45^-CD146^-$ cells were incubated for 48 h and washed to remove nonadherent cells. The purity of $EpCAM^+$ cells was 90–95%.

**Statistical Analysis.** The Kaplan–Meier product-limit method was used to obtain survival curves. Survival data were analyzed with the Mantel–Cox log-rank test. Overall GVHD clinical scores were analyzed using two-way ANOVA with a Tukey post hoc test. The Student's *t* test was used for the statistical analysis of real-time PCR or in vitro data. A $P$ value of $<0.05$ was defined as statistically significant. The data are presented as the mean ± SEM.

**ACKNOWLEDGMENTS.** This research was supported by the Basic Science Research Program through the National Research Foundation of Korea (NRF) funded by the Ministry of Education (NRF-2016R1D1A1B03934016 to S.-K.S.), the 2016 Creative Research Program of Inje University (S.-K.S.), and the 2016 Post-Doctoral Research Program of Inje University (S.-M.L.).

1. Taylor MW, Feng GS (1991) Relationship between interferon-gamma, indoleamine 2,3-dioxygenase, and tryptophan catabolism. *FASEB J* 5:2516–2522.
2. Curti A, Trabanelli S, Salvestrini V, Baccarani M, Lemoli RM (2009) The role of indoleamine 2,3-dioxygenase in the induction of immune tolerance: Focus on hematology. *Blood* 113:2394–2401.
3. Mellor AL, Munn DH (2004) IDO expression by dendritic cells: Tolerance and tryptophan catabolism. *Nat Rev Immunol* 4:762–774.
4. Grohmann U, Fallarino F, Puccetti P (2003) Tolerance, DCs and tryptophan: Much ado about IDO. *Trends Immunol* 24:242–248.
5. Munn DH, Mellor AL (2013) Indoleamine 2,3 dioxygenase and metabolic control of immune responses. *Trends Immunol* 34:137–143.
6. Bessede A, et al. (2014) Aryl hydrocarbon receptor control of a disease tolerance defence pathway. *Nature* 511:184–190.
7. Opitz CA, et al. (2011) An endogenous tumour-promoting ligand of the human aryl hydrocarbon receptor. *Nature* 478:197–203.
8. Kim H, et al. (2012) Brain indoleamine 2,3-dioxygenase contributes to the comorbidity of pain and depression. *J Clin Invest* 122:2940–2954.
9. Litzenburger UM, et al. (2014) Constitutive IDO expression in human cancer is sustained by an autocrine signaling loop involving IL-6, STAT3 and the AHR. *Oncotarget* 5:1038–1051.
10. Yanik GA, et al. (2008) The impact of soluble tumor necrosis factor receptor etanercept on the treatment of idiopathic pneumonia syndrome after allogeneic hematopoietic stem cell transplantation. *Blood* 112:3073–3081.
11. Varelias A, et al. (2015) Lung parenchyma-derived IL-6 promotes IL-17A-dependent acute lung injury after allogeneic stem cell transplantation. *Blood* 125:2435–2444.
12. Jamieson AM, et al. (2013) Role of tissue protection in lethal respiratory viral-bacterial coinfection. *Science* 340:1230–1234.
13. Arpaia N, et al. (2015) A distinct function of regulatory T cells in tissue protection. *Cell* 162:1078–1089.
14. Hayashi T, et al. (2004) Inhibition of experimental asthma by indoleamine 2,3-dioxygenase. *J Clin Invest* 114:270–279.
15. Desvignes L, Ernst JD (2009) Interferon-gamma-responsive nonhematopoietic cells regulate the immune response to Mycobacterium tuberculosis. *Immunity* 31:974–985.
16. Iannitti RG, et al. (2013) Th17/Treg imbalance in murine cystic fibrosis is linked to indoleamine 2,3-dioxygenase deficiency but corrected by kynurenines. *Am J Respir Crit Care Med* 187:609–620.
17. Romani L, et al. (2008) Defective tryptophan catabolism underlies inflammation in mouse chronic granulomatous disease. *Nature* 451:211–215.
18. Shakespear MR, Halili MA, Irvine KM, Fairlie DP, Sweet MJ (2011) Histone deacetylases as regulators of inflammation and immunity. *Trends Immunol* 32:335–343.
19. Reddy P, et al. (2004) Histone deacetylase inhibitor suberoylanilide hydroxamic acid reduces acute graft-versus-host disease and preserves graft-versus-leukemia effect. *Proc Natl Acad Sci USA* 101:3921–3926.
20. Reddy P, et al. (2008) Histone deacetylase inhibition modulates indoleamine 2,3-dioxygenase-dependent DC functions and regulates experimental graft-versus-host disease in mice. *J Clin Invest* 118:2562–2573.
21. Choi SW, et al. (2014) Vorinostat plus tacrolimus and mycophenolate to prevent graft-versus-host disease after related-donor reduced-intensity conditioning allogeneic haemopoietic stem-cell transplantation: A phase 1/2 trial. *Lancet Oncol* 15:87–95.
22. Choi SW, et al. (2015) Histone deacetylase inhibition regulates inflammation and enhances Tregs after allogeneic hematopoietic cell transplantation in humans. *Blood* 125:815–819.
23. Sun Y, et al. (2009) Cutting edge: Negative regulation of dendritic cells through acetylation of the nonhistone protein STAT-3. *J Immunol* 182:5899–5903.
24. Jasperson LK, et al. (2008) Indoleamine 2,3-dioxygenase is a critical regulator of acute graft-versus-host disease lethality. *Blood* 111:3257–3265.
25. Jasperson LK, et al. (2009) Inducing the tryptophan catabolic pathway, indoleamine 2,3-dioxygenase (IDO), for suppression of graft-versus-host disease (GVHD) lethality. *Blood* 114:5062–5070.
26. Bedoret D, et al. (2009) Lung interstitial macrophages alter dendritic cell functions to prevent airway allergy in mice. *J Clin Invest* 119:3723–3738.
27. Yi T, et al. (2009) Reciprocal differentiation and tissue-specific pathogenesis of Th1, Th2, and Th17 cells in graft-versus-host disease. *Blood* 114:3101–3112.
28. Mauermann N, et al. (2008) Interferon-gamma regulates idiopathic pneumonia syndrome, a Th17+CD4+ T-cell-mediated graft-versus-host disease. *Am J Respir Crit Care Med* 178:379–388.
29. Uryu H, et al. (2015) α-Mannan induces Th17-mediated pulmonary graft-versus-host disease in mice. *Blood* 125:3014–3023.
30. Burman AC, et al. (2007) IFNgamma differentially controls the development of idiopathic pneumonia syndrome and GVHD of the gastrointestinal tract. *Blood* 110: 1064–1072.
31. Grinyó JM, et al. (2004) Low-dose cyclosporine with mycophenolate mofetil induces similar calcineurin activity and cytokine inhibition as does standard-dose cyclosporine in stable renal allografts. *Transplantation* 78:1400–1403.
32. Kobayashi T, Momoi Y, Iwasaki T (2007) Cyclosporine A inhibits the mRNA expressions of IL-2, IL-4 and IFN-gamma, but not TNF-alpha, in canine mononuclear cells. *J Vet Med Sci* 69:887–892.
33. Choi SW, Reddy P (2014) Current and emerging strategies for the prevention of graft-versus-host disease. *Nat Rev Clin Oncol* 11:536–547.
34. Yuan ZL, Guan YJ, Chatterjee D, Chin YE (2005) Stat3 dimerization regulated by reversible acetylation of a single lysine residue. *Science* 307:269–273.
35. Franzke A, et al. (2003) G-CSF as immune regulator in T cells expressing the G-CSF receptor: Implications for transplantation and autoimmune diseases. *Blood* 102: 734–739.
36. Ciorba MA, et al. (2010) Induction of IDO-1 by immunostimulatory DNA limits severity of experimental colitis. *J Immunol* 184:3907–3916.
37. Orabona C, et al. (2006) Toward the identification of a tolerogenic signature in IDO-competent dendritic cells. *Blood* 107:2846–2854.
38. Puccetti P, Grohmann U (2007) IDO and regulatory T cells: A role for reverse signalling and non-canonical NF-kappaB activation. *Nat Rev Immunol* 7:817–823.
39. Pallotta MT, et al. (2011) Indoleamine 2,3-dioxygenase is a signaling protein in long-term tolerance by dendritic cells. *Nat Immunol* 12:870–878.
40. Coleman MM, et al. (2013) Alveolar macrophages contribute to respiratory tolerance by inducing FoxP3 expression in naive T cells. *Am J Respir Cell Mol Biol* 48:773–780.
41. Lemaître PH, et al. (2013) Cyclosporine A drives a Th17- and Th2-mediated post-transplant obliterative airway disease. *Am J Transplant* 13:611–620.
42. Novotny-Diermayr V, et al. (2010) SB939, a novel potent and orally active histone deacetylase inhibitor with high tumor exposure and efficacy in mouse models of colorectal cancer. *Mol Cancer Ther* 9:642–652.
43. Novotny-Diermayr V, et al. (2011) Pharmacodynamic evaluation of the target efficacy of SB939, an oral HDAC inhibitor with selectivity for tumor tissue. *Mol Cancer Ther* 10: 1207–1217.
44. Hill GR, et al. (1997) Total body irradiation and acute graft-versus-host disease: The role of gastrointestinal damage and inflammatory cytokines. *Blood* 90:3204–3213.
45. Markey KA, et al. (2012) Immune insufficiency during GVHD is due to defective antigen presentation within dendritic cell subsets. *Blood* 119:5918–5930.
46. Ma Y, et al. (2011) Contribution of IL-17-producing gamma delta T cells to the efficacy of anticancer chemotherapy. *J Exp Med* 208:491–503.
47. Yi T, et al. (2008) Absence of donor Th17 leads to augmented Th1 differentiation and exacerbated acute graft-versus-host disease. *Blood* 112:2101–2110.
48. Chuquimia OD, et al. (2012) The role of alveolar epithelial cells in initiating and shaping pulmonary immune responses: Communication between innate and adaptive immune systems. *PLoS One* 7:e32125.